Yin et al. Journal of Translational Medicine (2025) 23:239
https://doi.org/10.1186/s12967-024-05840-1

Journal of Translational Medicine

RESEARCH Open Access

Bone marrow fluid enhances the osteogenic activity of induced membrane leading to spontaneous osteogenesis: experimental validation and application in tibiofibular fusion for support reconstruction of segmental tibial defects

Qudong Yin[1†], Xueming Chen[1†], Shihao Du[1†], Xuming Wei[2], Yongwei Wu[1] and Fanyu Bu[1*]

Abstract

Background Managing large bone defects remains a significant clinical problem. We enhanced the osteogenic activity of the induced membrane (IM) by incorporating bone marrow fluid, leading to spontaneous osteogenesis (SO). We aimed to explore the application of this method in tibiofibular fusion (TFF) for reconstructing segmental tibial defects.

Methods Forty-two rats with femoral defects were divided into seven groups ($n=6$). Defects in groups A1-3 and B1-3 were filled with polymethylmethacrylate spacers while Group B4 was the control. Kirschner wires were used in Groups A1 and B1, plating was used in Groups A3 and B3-4, while the medullary canal was sealed in Groups A2 and B2. In Group A, osteogenic activity was measured using immunohistochemistry, W-B, and qRT-PCR. In Group B, the osteogenic results were measured using X-ray and gross examinations. Ten patients with 4–10 cm segmental defects of the middle and distal tibia underwent reconstruction using the IM technique, and IM and bone marrow fluid-induced SO for TFF, whose effects were assessed.

Results At five weeks, Group A1 showed higher levels of BMSCs and expression of BMP-2 and TGF-β1 than Groups A2 and A3 ($p<0.05$). After 12 weeks, Group B1 had more new bone at the bone end than Group B3 ($p=0.009$) whereas Groups B2 and B4 did not. All tibial defects and TFF healed. The TFF site and posterior tibia healed faster than the other sides and showed quicker clinical healing ($p<0.05$). All patients could fully bear weight before tibial clinical healing, with an excellent-to-good functional rate of 80% (Paley's criterion) at the 13 – to 36-month follow-up.

†Qudong Yin, Xueming Chen, Shihao Du Contributed equally to this work.

*Correspondence:
Fanyu Bu
bofanyuyqd@163.com

Full list of author information is available at the end of the article

Conclusion Bone marrow fluid enhances the osteogenic activity of IMs leading to SO. TFF by SO progresses faster than tibial clinical healing, making the IM technique an effective stabilizer for faster and better functional recovery after reconstruction of segmental defects of the middle and distal tibia.

Keywords Bone defect, Induced membrane, Tibiofibular fusion, Spontaneous osteogenesis, Bone marrow

Background

Segmental tibial defects are commonly encountered in clinical practice. The primary approach for their reconstruction involves using the Masquelet-induced membrane technique (IMT) [1–3]. This technique consists of a two-stage surgical procedure. In the first stage, surgeons perform radical debridement and insert a cement spacer made of polymethylmethacrylate (PMMA) into the bone defect. During the second stage, the spacer is removed, leaving the induced membrane (IM) in place, and the cavity is filled with an autograft. In standard IMT, both staged surgery and bone grafting are necessary [3, 4]. IMs not only act as a protective physical barrier, preventing autograft resorption but also function as bioreactors. They promote osteogenesis through revascularization, growth factor secretion, and the concentration of bone mesenchymal stem cells (BMSCs) [3–6]. In other words, IMs exhibit intrinsic osteogenic activity, making the IMT highly effective in treating segmental tibial defects. In 2009, Klaue et al. [7] observed a small amount of new bone formation in the IM near the bone end after 8–12 weeks of filling femoral defects in animals with PMMA. Similarly, in 2013, Gruber et al. [8] reported similar findings. In 2023, Yin et al. [9] introduced the term "induced membrane spontaneous osteogenesis" (IMSO) to describe new bone formation within IM without relying on material bone grafts. At the same time, they reported varying degrees of IMSO in a few cases. Due to the reparative properties of autologous bone marrow fluid, which contribute to healing of segmental bone defect, Yin et al. hypothesized that bone marrow fluid from the bone end enhances the osteogenic activity of the IM, potentially leading to SO. However, this hypothesis has not been adequately tested. Nevertheless, the IMSO phenomenon enables the performance of one-stage surgery or the use of fewer or no bone grafts for repairing bone defects with the improved IMT.

Tibiofibular fusion (TFF) is an effective surgical approach for patients with poor bone stock, complex nonunion, and large segmental tibial defects [10–13]. This effectiveness has led many scholars to suggest an auxiliary stabilizing role of TFF while repairing segmental tibial defects with IMT. For classic TFF, a material bone graft is necessary above the distal tibiofibular syndesmosis (DTFS). In contrast, IMSO-induced TFF does not require such a graft. Consequently, this enhanced technique appears superior to classic TFF, representing a viable strategy for reconstructing segmental tibial defects.

Therefore, we developed the induced membrane and bone marrow fluid-induced tibiofibular fusion (IMBMFITFF) technique to support the reconstruction of segmental tibial defects treated using IMT. To our knowledge, IMBMFITFF for this type of reconstruction has not been reported in the literature. This study aimed to validate IMSO and evaluate the effectiveness of IMBMFITFF.

Methods

Study design

This experimental study was reviewed and approved by the Institutional Animal Care and Use Committee of our Hospital. We adhered to the ARRIVE guidelines and included the ARRIVE checklist. Our retrospective clinical study also received approval from the Ethics Committee of our Hospital and was consistent with the ethical standards outlined in the 1964 Declaration of Helsinki and its subsequent amendments. Written informed consent for participation in the study was obtained from each patient.

Animal experiment

Grouping and housing conditions of the animals

Forty-two 8–10 week specific pathogen-free adult male Sprague–Dawley rats (mean weight 281 g, range 245–305 g) were randomly divided into seven groups ($n = 6$). Group A, including A1, A2, and A3, was used to assess the osteogenic activity of the IM under different fixation methods, which represent varying volumes of bone marrow overflow, including a Kirschner wire (more bone marrow overflow), medullary canal sealing (no bone marrow overflow), and a plate (less bone marrow overflow). Meanwhile, Group B, including B1, B2, B3, and B4, was employed to observe the osteogenic outcomes related to the previously mentioned different fixation methods. Group B4 served as the bone defect control group. After one week of acclimation in the animal experiment center [temperature: 20–23 °C; the day/night light cycle: 12 h/12 h; humidity: 60–80%; sterile complete feed (Anlimo, Nanjing, China) and filtered water were freely available].

Surgical procedure 5% pentobarbital (45 mg/kg) was injected intraperitoneally to induce general anesthesia. The surgical area was shaved and disinfected with iodophor. A 3-cm incision was made in the skin and muscles on the dorsal side parallel to the long axis of the right

femur, and the subcutaneous muscles were dissected to expose its surface. Two osteotomies were performed using a swing saw to remove a 10-mm mid-diaphyseal fragment [6, 9]. Bone defects were filled with in vitro-prepared PMMA spacers of the corresponding size. In Groups A1, A2, B1, and B2, 1.4 mm K-wires were used for an intramedullary fixation through the spacer. In Groups A3, B3, and B4, small steel plates were used for internal fixation (Huachuang Medical, ALPS titanium alloy pet orthopedic instruments). In Groups A2 and B2, bone cement secured the junction of the spacer to the bone end, effectively sealing the medullary canal. In Group B3, the cement spacers were sutured to the plate. Figure 1. The incisions were rinsed with physiological saline. The muscles were repositioned and the incisions closed using bioresorbable sutures. To prevent infection, intramuscular injections of 4×10^4 U of penicillin sodium were given within three days of the operation. Throughout the recovery period, the animals were closely monitored, and co-housed in a single cage until their surgical incisions healed.

Osteogenic activity analysis

Rats in Groups A1, A2, and A3 were euthanized with an overdose (130 mg/kg) of pentobarbital administered intraperitoneally at five weeks after surgery. The animals were then routinely disinfected, spread on towels, and opened along the initial surgical site. The IMs around the spacers were harvested by separating the surrounding muscles. The IM samples in Groups A1, A2, and A3 were divided into two parts. Half of these samples were fixed in 4% paraformaldehyde and placed in cryopreservation tubes, which were then immediately stored in liquid nitrogen to assess the number of BMSCs. The remaining half of the IMs was used for measuring protein and mRNA expression of related factors.

BMSC count

The levels of BMSCs in the IMs were evaluated using a quantitative immunohistochemical method that detects STRO-1-positive cells [14]. The sections were incubated with mouse anti-rat STRO-1 (3 h; MAB1038, R&D Systems, Wiesbaden, Germany). Optical density analysis of the images was performed using ImageJ software. Three randomly selected fields of view were used to measure the optical density of STRO-1-positive cells. Subsequently, the data were analyzed using Prism Graph 6.0 software. The number of BMSCs in the IMs was counted using immunohistochemistry by detecting STRO-1-positive cells.

Western blotting

Frozen samples were processed for Western blotting to measure the expression of bone morphogenetic protein-2

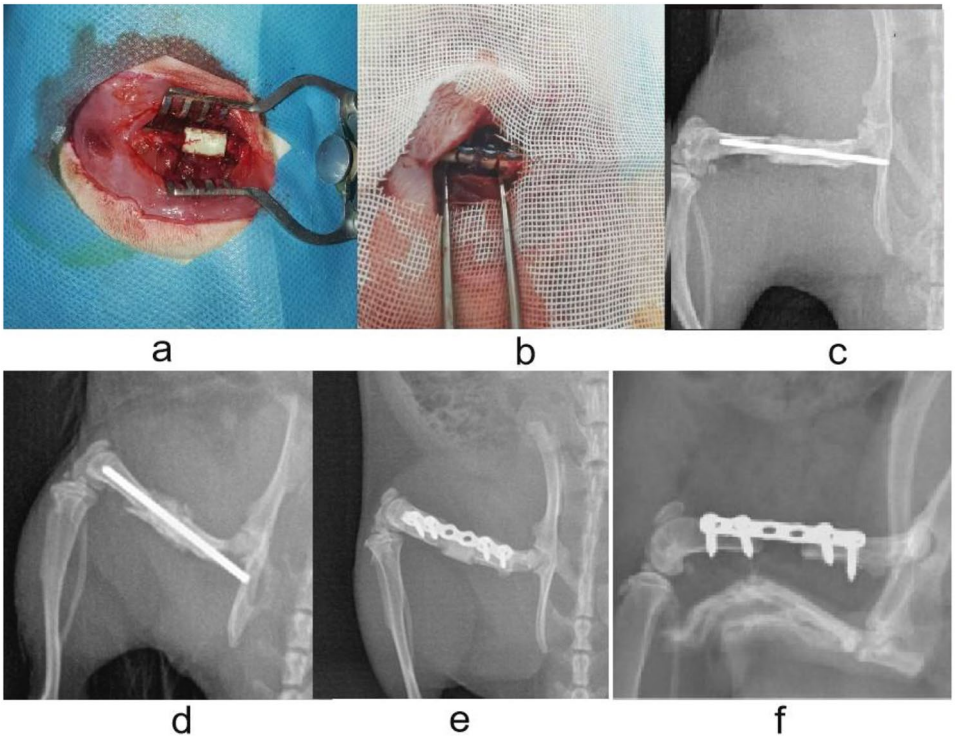

Fig. 1 Grouping and fixation types of bone defects in the right femur in rats. (**A**) The bone defect was fixed using a Kirschner wire. (**B**) The bone defect was fixed using a plate. (**C**) X-rays of Groups A1 and B1 fixed with Kirschner wires. (**D**) X-rays of Groups A2 and B2 with medullary canal sealing. (**E**) X-rays of Groups A3 and B3 fixed with plates. (**F**) X-ray of Group B4 with a blank control

(BMP-2), transforming growth factor β1 (TGF-β1), and vascular endothelial growth factor (VEGF) protein. Proteins were extracted from IMs using RIPA lysis buffer (Beyotime Institute of Biotechnology, Nantong, China) and quantified by the BCA Protein Assay Kit (Beyotime Institute of Biotechnology). The protein extract was subjected to SDS-PAGE gel electrophoresis and transferred to polyvinylidene fluoride (PVDF) membranes. The PVDF membranes containing target bands were incubated overnight in the corresponding primary antibodies at 4℃. After an hour of incubation of the secondary antibodies of the corresponding species, the target bands were detected using the CFX96 Real-Time System (Bio-Rad, America). Quantification of the blots was performed using ImageJ software, and the expression levels of the target proteins were normalized to β-actin. The following antibodies were used: BMP-2 (ab214821; Abcam), TGF-β1 (ab215715; Abcam), and VEGF (ab46154; Abcam).

Quantitative real-time polymerase chain reaction (qRT–PCR)

The IM tissue was removed from the cryopreservation tube, and qRT−PCR was used to measure the mRNA expression of BMP-2, TGF-β1, and VEGF. Total RNA was extracted using Trizol Reagent (Thermo Fisher Scientific, Waltham, MA, USA) and reverse-transcribed into cDNA. qRT-PCR was performed using UltraSYBR Mixture (Jiangsu CoWin Biotech, Co., Ltd., Beijing, China). The expression of each gene was normalized to that of the housekeeping gene, GAPDH, in a selected control sample. The following primer sequences were used: VEGFA, Forward 5′-TCCTGTGTGCCCCTAATGC-3′ and Reverse 5′-ACGCACTCCAGGGCTTCAT-3′; BMP-2, Forward 5′- CTTTTGGCCACGACGGTAAA-3′ and Reverse 5′-TGCCTTTTGCAGCTGGACTT-3′; TGF-β1, Forward 5′-GACTCTCCACCTGCAAGACCAT-3′ and Reverse 5′-GGACTGGCGAGCCTTAGTTTG-3′; GAPDH, Forward 5′- GTATGACTCTACCCACGGCA AGT-3′ and Reverse 5′- TCTCGCTCCTGGAAGATGG T-3′.

Osteogenic outcomes

Rats in Groups B1, B2, B3, and B4 were euthanized after 12 weeks postoperatively for radiographic and gross examinations to assess new bone formation of the IMs. The length of new bone formation was defined as the average of the longest distances from the proximal and distal bone ends to the center of the bone defect, measured either by X-ray examination or visual inspection.

Clinical application

Inclusion and exclusion criteria

Inclusion criteria: (1) Patients with segmental defects of the middle and distal tibia treated with IMT for tibial defects and IMBMFITFF for TFF in our hospital; (2) Patients aged > 15 years; (3) Patients with a follow-up time of > 12 months. Exclusion criteria: (1) Patients with malignant tumors, immunocompromised conditions, or acquired immunodeficiency syndrome; (2) Patients with postoperative infection; (3) Patients with incomplete clinical or follow-up data.

General information

Between January 2018 and May 2023, ten patients met the inclusion criteria. All of them had traumatic fractures with bone defects. Among these patients, there were seven males and three females; aged between 25 and 68 years, with an average age of 46.8 years.

Therapeutic methods

The surgery was performed in two stages.

Stage one:

(1) Debridement: Preoperative imaging and visual assessment were used to identify bone areas and soft tissue necrosis. Usually, the anterior lateral incision approach of the calf was used. Debridement was performed until the "paprika sign" was observed, indicating bleeding and viable bone at the resection margin. Necrotic tissue, sequestra, and old fixations were completely removed. After debridement, the wound was regularly irrigated with a large volume of hydrogen peroxide and normal saline. Subsequently, the surgical area was again disinfected again with iodophor. Finally, the operating sheet was replaced, and surgical instruments were prepared.
(2) Stabilization of the tibial bone defect: PMMA cement spacers were inserted into the tibial defects as well as between the tibia and fibula. Depending on the defect location and infection risk, plates, intramedullary nails, or external fixators were used to restore normal limb length and alignment. After filling the defects with PMMA bone cement, the wound was closed. In challenging cases (seven instances), skin flap repair was necessary. Perforator flaps were preferred in five cases, and free anterolateral thigh flaps in two cases. Deep drainage was also performed.
(3) Postoperative management: Antibiotics were administered for three days post-surgery.

Stage two:

After the initial stage, staged IMT was performed 6–12 weeks later, with no infection symptoms and normal primary laboratory indicators. During the second stage, in all patients, we performed autologous iliac bone grafting through the anterior lateral approach at the tibial bone defect site, avoiding extension into the tibiofibular space. Skeletal stabilization was achieved either using either

internal fixation (in seven cases) or external fixation (in three cases). Meanwhile, we dipped several hemostatic sponge pieces into bone marrow fluid at the iliac bone graft harvesting site and placed them into the IM between the tibia and fibula. Finally, we inserted deep drainage and sutured the incision closed.

Postoperative management and follow-up

Intravenous antibiotics were administered for five days postoperatively. Functional exercises were initiated one week after operation. Imaging examinations and outpatient interviews were conducted every month before clinical healing of the tibial defect and every three months thereafter.

Evaluation

Evaluation involved observing initial and full weight-bearing times, as well as healing times for specific tibial regions: anterior, posterior, medial, and lateral sides, including the TFF site. We also assessed clinical healing time, complications, and functional recovery. Radiographically, the appearance of new bone bridging indicated healing either of the bone defect on that side or of the TFF. The imaging standard for clinical healing of tibial defects is the presence of new bone bridging on at least three of the four sides, or covering 75% of the circumference. Given that limb function generally stabilizes 2 years after reconstruction surgery, the longest follow-up period in this study was 3 years. Limb function was assessed in accordance with Paley's criteria [15].

Statistics

Data with normal distribution are presented as mean ± standard deviation. Statistical analysis was performed by one-way ANOVA using SPSS 26.0 software (SPSS, Inc., Chicago, IL, USA), followed by a post-hoc analysis with Bonferroni's test for data with a normal distribution. For data with a nonnormal distribution, we used the nonparametric Kruskal-Wallis test. A $p < 0.05$ (two-tailed) was considered statistically significant.

Results

Experimental outcomes

BMSC counts

BMSC counts showed significant differences among the three groups at 5 weeks. Specifically, Group A1 had more BMSCs than Groups A2 and A3, with a significant difference ($p < 0.05$). Figure 2.

Western blotting

The gray value and protein expression levels of BMP-2 and TGF-β1 significantly differed at 5 weeks among the three groups. Specifically, Group A1 exhibited significantly higher gray values and protein expression levels compared to Groups A2 and A3 ($p < 005$). However, the gray value and protein expression level of VEGF at 5 weeks did not differ among the three groups ($p > 0.05$). Figure 3.

qRT–PCR

At 5 weeks, Group A1 had significantly higher mRNA levels of BMP-2 and TGF-β in the IMs, compared to Groups A2 and A3 ($p < 0.05$). However, the mRNA level of VEGF did not differ among the three groups ($p > 0.05$). Figure 4.

Osteogenic outcomes

X-ray examinations and gross observations after 12 weeks revealed the following: (i) The IMs in Group B1 were thicker and harder, with a distinct lip-shaped new bone growth originating from the bone end, and expanding along the IM. In two specimens, the new bone extended to the middle of the bone defect. The length of new bone formation ranged between 2 mm and 6 mm, with an average of 3.4 ± 0.4 mm. However, the new bone was uneven, with more new bones formed proximally to the bone defect and on the contralateral side of the incision. (ii) The IMs in Group B2 neither thickened nor hardened, and bone atrophy was observed at the bone end. (iii) The gap between the cement spacer and the bone end in Group B3 partially disappeared, and only a small amount of new bone formation was observed at the bone end, the length of new bone formation ranged between 0 and 2 mm, with an average of 0.5 ± 0.1 mm. (iv) The bone ends of Group B4 were wrapped in soft tissue, leading to bone resorption and bone atrophy. The new bone formation amount was significantly different between the four groups ($F = 27.437$, $p < 0.01$). Specifically, in Group B1, more new bone was formed than in Group B3 ($t = 3.126$, $p = 0.009$), and, similarly, more new bone was observed in Group B3 than in Groups B2 and B4 ($t = 9.948$, $p < 0.001$). Figure 5.

The flowchart summarizing the experimental design and the main findings for each group summary results are shown in Fig. 6.

Clinical outcomes

All patients were monitored for 13–36 months, with an average of 20 months. The initial weight-bearing time was 6.5 weeks (range, 4–13 weeks), and the full weight-bearing time was 8.9 months (range, 7–12 months). All bone defects healed with a clinical healing time for the tibia of 10.9 ± 2.2 months (range, 8–13 months). However, there was one case where a loss of the anterior tibial cortex was observed. The TFF occurred in all cases. The healing times at different sites, listed in ascending order, were as follows: the posterior side (8.00 months), TFF site (8.50 months), lateral side (9.30 months), tibial clinical

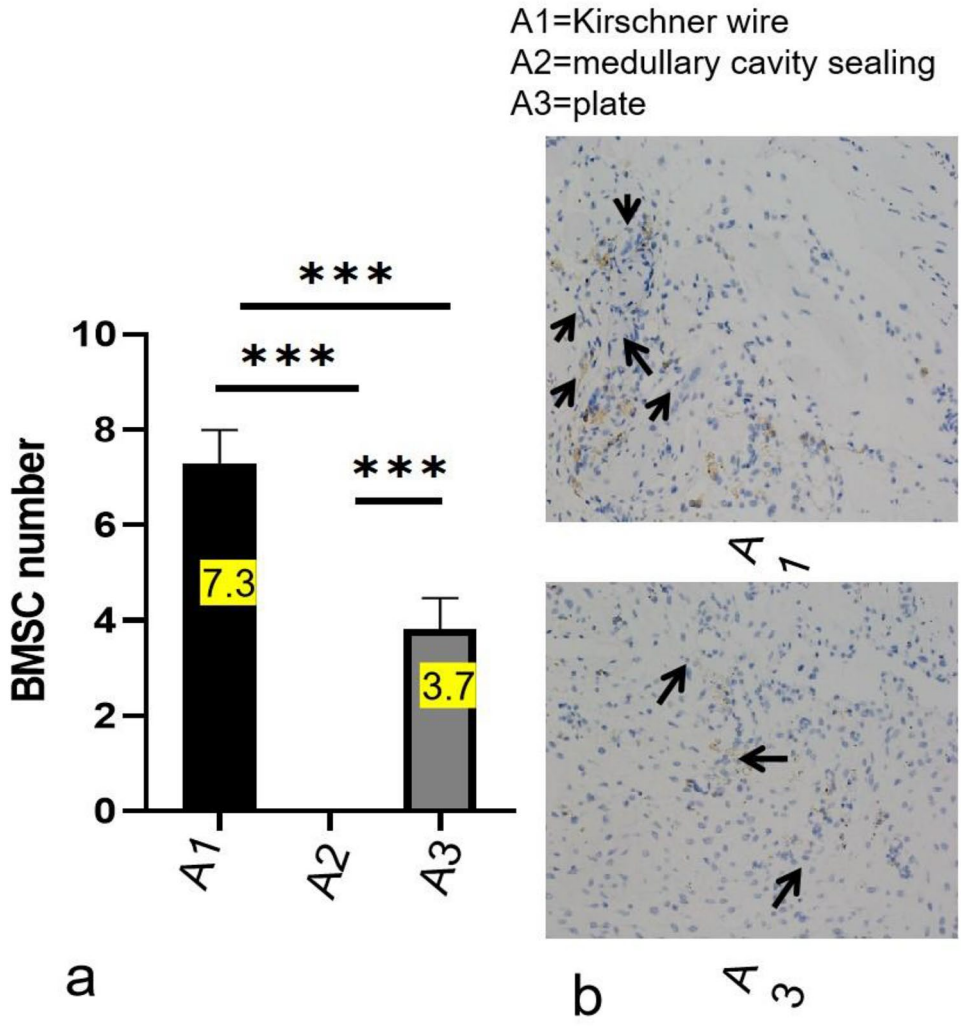

Fig. 2 Comparison of BMSC concentration at 5 weeks. (**A**) Comparison of the columns based on the relative BMSC numbers. (**B**) Group A1 had more BMSCs (STRO-1+ cells) than Group A3 (× 200). Note: black arrow, BMSC; ***$p < 0.001$

healing (9.70 months), medial side (9.90 months), and anterior side (10.11 months). These showed significant differences ($F = 5.799$, $p < 0.05$). Notably, the healing time of the posterior side and TFF site was shorter than that of the anterior and tibial clinical healing ($p < 0.05$). Figure 7. There were no postoperative infections. At the final follow-up, all patients were satisfied with the functional recovery of their lower limbs. Based on Paley's score, the excellent-to-good rate for functional recovery was 80%. A typical case is shown in Fig. 8.

Discussion

Causes of IMSO and IMBMFITFF

Giannoudis's "diamond concept" has gained worldwide recognition for identifying essential elements required for successful repair of bone defects and nonunions [16]. These elements include osteoinductive mediators, osteoconductive matrix (scaffold), osteogenic cells, an optimal mechanical environment, sufficient blood supply, and resolution of host comorbidities. The absence of any of these elements prevents fully functional reconstruction of bone defects and nonunions. IMs encompass all key elements of the "diamond concept." Since they function in close proximity to the bone end, they serve as: (i) osteoinductive mediators: IMs contain osteogenic and angiogenic factors such as BMP-2, TGF-β1, and VEGF [3, 8]; (ii) osteoconductive matrix: IMs act as biological scaffolds that mediate the attachment of cells and factors. This separation prevents atrophy or absorption without new bone formation, as observed in control group [17, 18]; (iii) osteogenic cells: IMs contain multiple cell types, especially BMSCs [14]; (iv) the surface of IMs is rich in microvessels, contributing to the growth of new bone tissue; (v) an optimal mechanical environment is maintained by either internal or external fixation. Therefore,

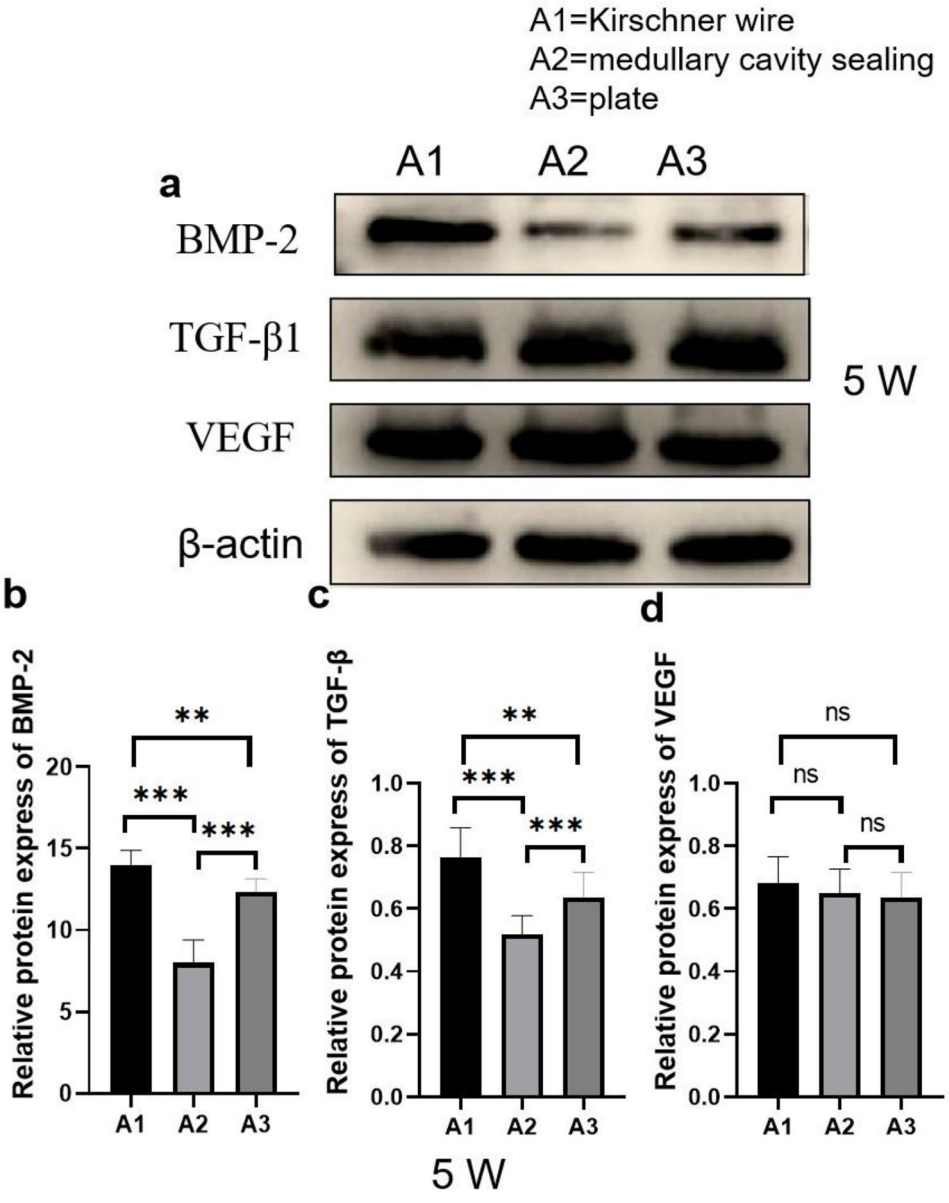

Fig. 3 The expression of osteogenic and angiogenic factor proteins in each group of induced membranes by Western blot analysis at 5 weeks. (**A**) Western blot images of BMP-2, TGF-β1, and VEGF for each group of induced membranes. (**B-D**) Relative quantification of Western blot bands corresponding to different factors. Note: ns, not statistically significant; $^{**}p < 0.01$; $^{***}p < 0.001$

IMs near the bone end exhibit intrinsic osteogenic activity and BMSC presence, enabling SO.

Although BMSCs can originate from the bone marrow and periosteum at the bone end, their primary source is the bone marrow. Our experimental study confirmed that bone marrow fluid can enhance the osteogenic activity of the IM, and that BMSCs in the bone marrow fluid are crucial for IMSO. As in our study, experiments on IMT conducted by Henrich et al. [14] confirmed the differences in IMs formed in soft tissues, such as subcutaneous tissues and muscles, compared to those around bone defects. IMs around femur defects had significantly elevated levels of BMP-2, TGF-β, and VEGF compared to IMs in soft tissues. The IMs around bone defects also contained BMSCs, which were absent in the soft tissue IMs. Pelissier et al. [19] and Catros et al. [20] also conducted experimental studies on IMT and have found that there are no osteoinductive effects in subcutaneous-induced membranes. The stimulation from the K-wire during lower-limb activity increases bone marrow fluid overflow, resulting in a higher number of BMSCs in Group A1, compared to Groups A2 and A3. Consequently, more new bone was formed in Group B1 than in Groups B2 and B3. Additionally, IMSO always grows

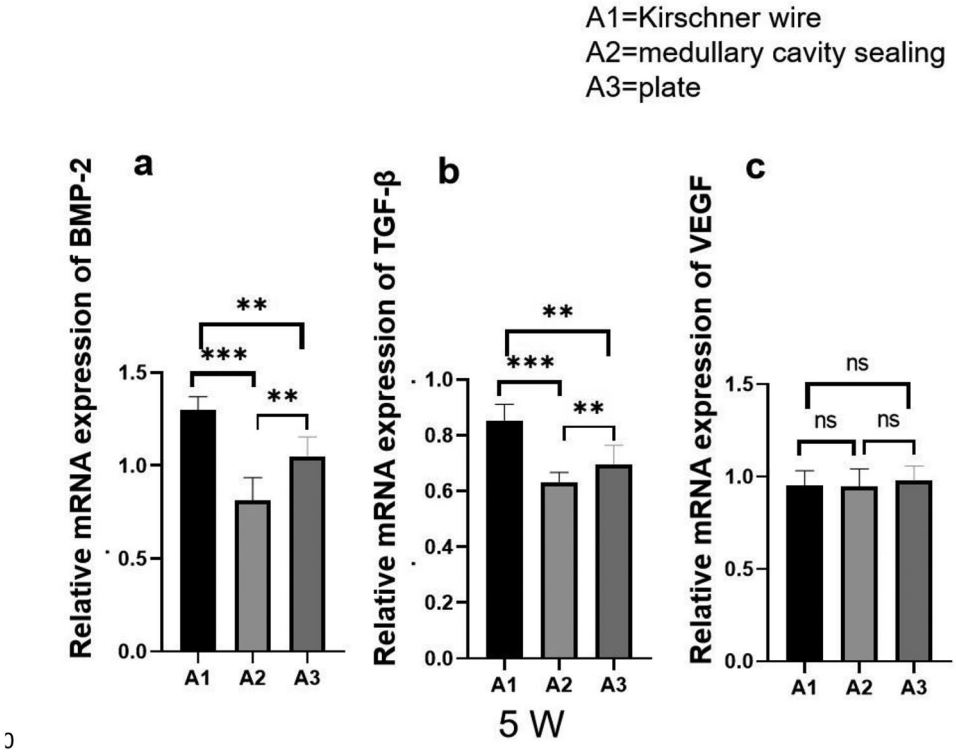

Fig. 4 The expression of osteogenic and angiogenic factor genes in each group of induced membranes by qRT-PCR at 5 weeks. (**A**) Relative quantification of mRNA expression of BMP-2 by qRT-PCR in each group of induced membranes. (**B**) Relative quantification of mRNA expression of TGF-β1 by qRT-PCR in each group of induced membranes. (**C**) Relative quantification of mRNA expression of VEGF by qRT-PCR in each group of induced membranes. Note: ns, not statistically significant; $^{**}p < 0.01$; $^{***}p < 0.001$

from the bone end to the center of the defect, consistent with the findings of Klaue et al. [7] and Gruber et al. [8]. All these observations indicate that bone marrow liquid can enhance the osteogenic activity of IMs, inducing SO, confirming a correlation between the amount of IMSO and the number of BMSCs from bone marrow fluid.

Our experimental study confirmed that bone marrow fluid can enhance the osteogenic activity of the IM, and BMSCs in bone marrow fluid are crucial for IMSO. Similarly to our findings, Henrich et al. [14] conducted an experimental study on IMT and found that there were differences in IMs formed in soft tissues, such as subcutaneous tissues and muscles, compared to those around bone defects; IMs around femur defects had significantly elevated levels of BMP-2, TGF-β, and VEGF compared to IMs in soft tissues; The IMs around bone defects also contained BMSCs, which were absent in soft tissue IMs. Pelissier et al. [19] and Catros et al. [20] also conducted experimental studies on IMT and have confirmed that there are no osteoinductive effects in subcutaneous-induced membranes. The stimulation from the K-wire during lower-limb activity increases bone marrow fluid overflow, resulting in a higher number of BMSCs in Group A1 compared to Groups A2 and A3. Consequently, more new bone was formed in Group B1 than in Groups B2 and B3. Additionally, IMSO always grows from the bone end to the center of the defect, consistent with the findings of Klaue et al. [7] and Gruber et al. [8]. All these observations indicate the bone marrow liquid can enhance the osteogenic activity of IMs, inducing SO, and there is a correlation between the amount of IMSO and the number of BMSCs from bone marrow fluid.

Bone marrow fluid contains osteogenic progenitor cells, such as multipotent hematopoietic stem cells and BMSCs, which both originate and reside in the bone marrow. These cells respond to specific stimuli to migrate, proliferate, and differentiate into specialized cells. Additionally, the bone fluid contains multiple growth factors, with signaling factors such as BMPs being secreted by BMSCs and endothelial cells to regulate the proliferation, differentiation, and migration of various bone-forming cells [21]. Therefore, bone marrow fluid represents an attractive means of facilitating bone repair. Percutaneous bone marrow injections as a standalone treatment method for delayed unions or nonunions resulted in long bone bridging in about 70% of patients [22]. One of the main reasons for the unsatisfactory healing rate is that bone marrow fluid cannot accumulate at the fracture site [22]. IMBMFITFF combining IM and bone marrow fluid through IM and sponge pieces, accumulates a large

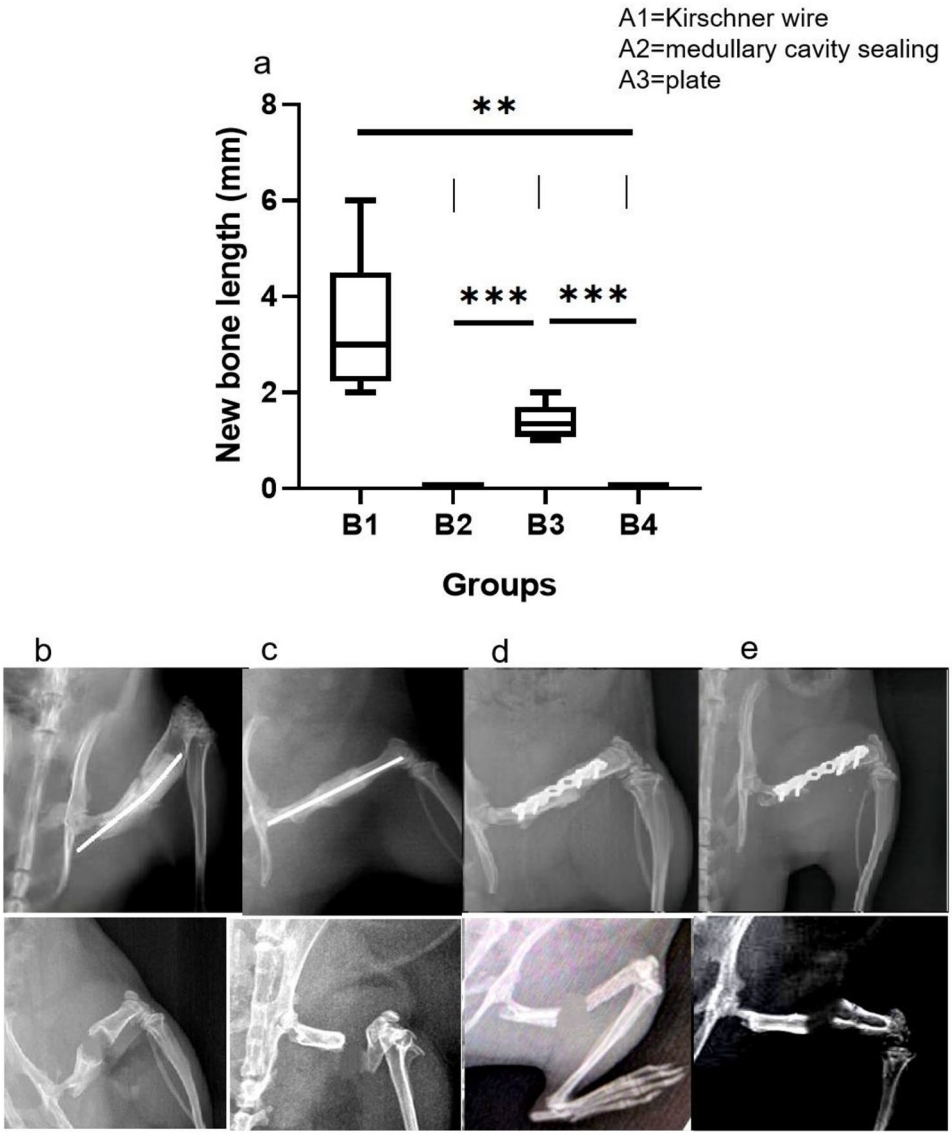

Fig. 5 X-ray images after 12 weeks post-surgery. (**A**) Comparison of the amount of new bone formation in different groups. (**B**) Significant new bone growth from the bone end towards the center of the bone defect, forming a lip-shaped wrapped bone cement spacer in Group B1. (**C**) No bone growth was observed in Group B2. (**D**) In Group B3, a small amount of new bone grew at the bone end. (**E**) In Group B4, atrophy was observed at the bone end. Note: $^{**}p < 0.01$; $^{***}p < 0.001$

amount of bone marrow fluid containing active ingredients (osteogenic cells and osteogenic factors) at the treated bone defects, producing a $1 + 1 > 2$ effect, promoting bone healing and achieving TFF.

Asymmetrical healing

Our data suggest asymmetrical healing of tibial defects, with the shortest healing time at the posterior side, followed by the lateral and medial sides, and finally the anterior side. Liu et al. [23] also observed asymmetrical growth of regenerated callus in patients with femoral defects treated using distraction osteogenesis. Our results agree with their findings that the posterior cortex was growing faster and exhibited a higher pixel value ratio than the medial, lateral, and anterior sides. Since the fibula and tibiofibular gap are located at the back of the tibia, the TFF heals faster, as does the posterior side of the tibia. Several factors contribute to this accelerated healing of the posterior side: (i) asymmetrical muscle coverage, with more extensive muscle coverage and blood supply in the posterior and lateral tibia, and between the tibia and fibula; (ii) gravitational sinking, leading to more bone grafts and bone marrow at the posterior part of the tibia and TFF site; (iii) different mechanical environment of bone grafts, with bone grafts located in the front being more susceptible to external forces. Additionally, the

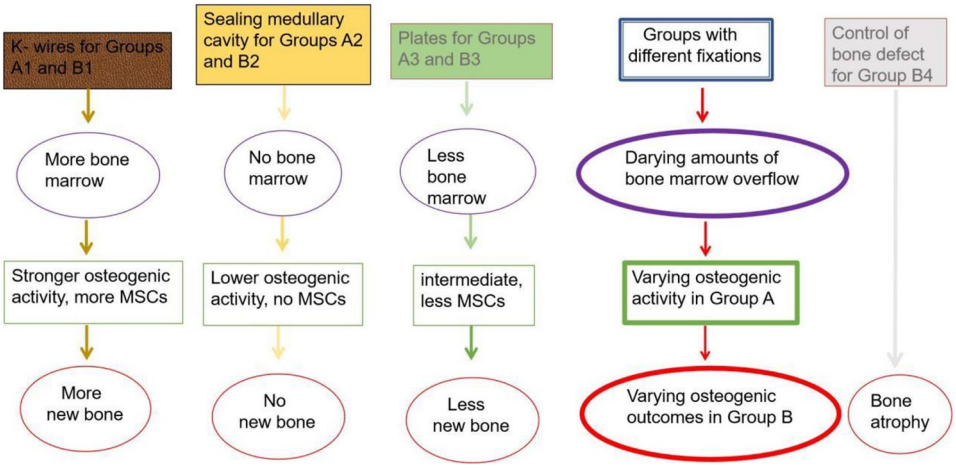

Fig. 6 Flowchart summarizing the experimental design and the main findings for each group

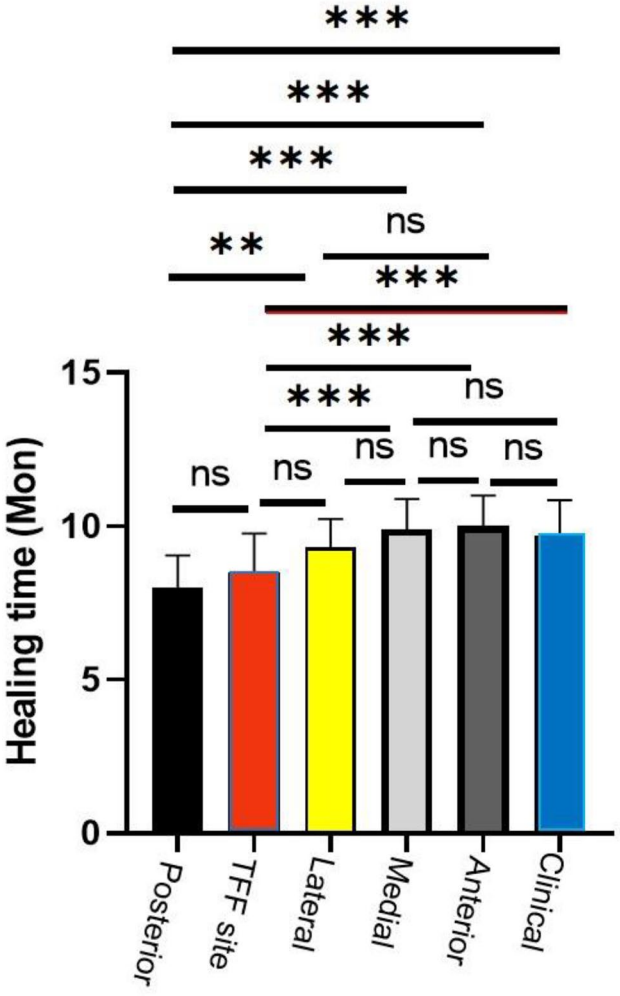

Fig. 7 Comparison of healing times at different sites. Note: ns, not statistically significant; $^{**}p < 0.01$; $^{***}p < 0.001$

incision is usually made at the front, where the IM may be incomplete. Consequently, the unfavorable mechanical environment of the anterior bone grafts can easily lead to graft dispersion, loss, or resorption. Especially during the early stages of bone healing, if out-of-bed activity occurs too early or is excessive, the stability of the bone grafts diminishes, making bone resorption and sinking more likely. In clinical practice, one patient who experienced loss of the tibial anterior side had excessive out-of-bed activity. Bone healing time correlates with factors such as the quantity of bone grafts or bone marrow, blood supply, and the mechanical environment [24–26]. Consequently, the TFF site and the tibial posterior exhibit faster healing compared to other areas.

Application effect and advantages of IMBMFITFF

TFF can be performed at or above the DTFS, without adversely affecting the ankle joint. A literature review by Lim et al. [12] has found no significant difference between syndesmosis fusion and ligament reconstruction for DTFS injuries. Magin [10] has found TFF especially effective in the treatment of a complicated tibial nonunion, while Choi et al. [26] suggest "4-in-1 osteosynthesis," which includes TFF, for an atrophic-type congenital pseudarthrosis of the tibia. Piątkowski and Modrzewski [11] have proposed TFF for the treatment of infected and difficult tibial pseudarthroses. Masquelet et al. [26] on the other hand, recommend TFF for large segmental tibial defects that had been treated using IMT. In essence, TFF can be an effective method for treating nonunions, large segmental tibial defects, DTFS injuries, instabilities, or comorbidities without producing adverse consequences [10–13, 27–29]. However, the classic TFF mentioned above requires bone grafts or/and internal fixation.

The enhanced IMT in this study has several advantages: (1) IMBMFITFF maintains consistent strength, alignment, and length of the lower limb, provides

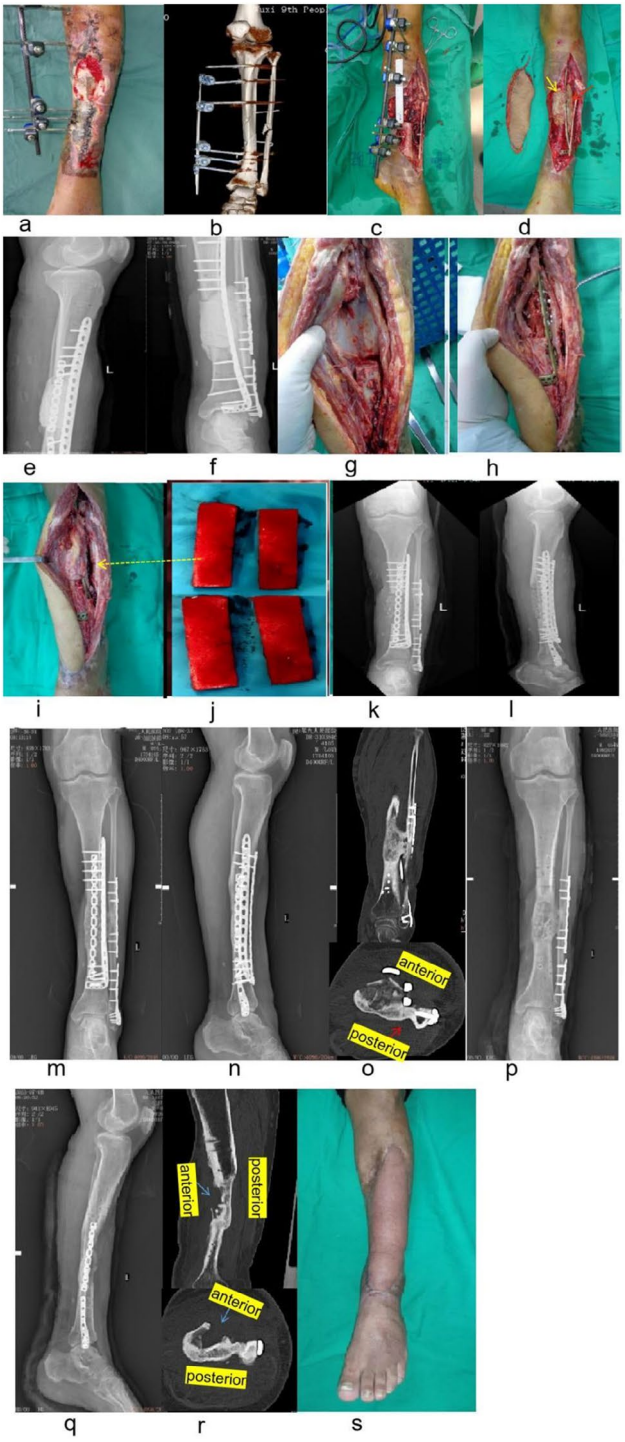

Fig. 8 A 54-year-old male patient with tibial defects treated using IMT and IMBMLITFF. (**A**) The appearance and (**B**) CT reconstruction revealed fractures of the tibia and fibula, along with soft tissue necrosis and defects. (**C**) After debridement, there were large segmental tibial and soft tissue defects. (**D**) PMMA spacers were independently inserted into the tibial defect (yellow arrow) and between the tibia and fibula (red arrow), and a free anterolateral femoral skin flap was used to repair the wound. (**E**, **F**) X-rays showed the cement spacers placed in the tibial defect and between the tibia and fibula. (**G**) During the second stage of the IMT, the spacer was removed. (**H**) Autologous bone was grafted at the tibial defect. (**I**, **J**) Several hemostatic sponge pieces, soaked in bone marrow fluid from the iliac bone graft harvesting site, were inserted into the IM space between the tibia and fibula. (**K**, **L**) Instant X-rays, after the second stage IMT procedure showed uniform bone grafting. (**M**, **N**) X-rays and (**O**) CT scans at 8 months postoperatively showed callus bridging the posterior tibial side and the TFF site, but not the anterior tibial and medial sides. (**P**, **Q**) X-rays and (**R**) CT scans at 12 months postoperatively showed clinical healing of the tibial defects, with a loss of the anterior tibial cortex. (**S**) The appearance at 12 months postoperatively shows good function

additional stability for large defects of the middle and distal tibia defects, and facilitates earlier weight-bearing. Compared to the proximal and middle tibial segments, the segment of the middle and distal lower tibia healed more slowly and was prone to non-union. Patients with the defects of the middle and distal treated with IMT without TFF can fully bear weight only after their tibia has clinically healed, resulting in longer waiting periods before returning to work and routine daily activities, and an unsatisfactory functional recovery. In contrast, patients receiving TFF can fully bear weight before the clinical healing of their tibia, thereby facilitating early functional recovery, provided that both TFF and the distal and lateral sides of the tibia have healed, due to the faster healing rates of TFF and increased stability. (2) No increase in surgical trauma and treatment costs since IMBMFITFF does not require material bone grafts nor internal fixation, making it easy to implement. It is noteworthy that the bone marrow fluid at the ilium harvest site from the previous iliac bone grafting did not produce the desired results. (3) IMBMFITFF itself has no adverse consequences [10–12, 26]. Gupta G, et al. [30] reported 9 patients with an average of 5.2 cm (range 3.3–8.5 cm) segmental tibial defects treated using IMT, the union time was 10.5 months (range 8–13 months). In ten cases, we performed IMBMLITFF to facilitate the reconstruction of segmental defects in the middle and distal tibia, achieving a TFF success rate. The average clinical healing time for the tibial defects was 10.9 months, with a range of 8–13 months), which aligns with findings from other studies [3, 30]. However, all patients were able to fully bear weight before the tibial defects clinically healed as well as the TFF and healing of the posterior-lateral tibia. This was because the healing of posterior-lateral tibia was quicker than the clinical healing, resulting in an excellent-to-good rate of 80% for functional recovery. No adverse effects were noted for IMBMFITFF.

Limitations and future directions

This study has some limitations. First, IMBMFITFF has not been conducted in in vivo animal models. Second, STRO-1 positivity is not the only definitive marker for BMSC. Third, the significant enhancement of osteogenic activity of the IM by the bone marrow is not well understood due to a lack of studies on the molecular mechanism. Fourth, a relatively small number of cases has been examined. Further research is necessary to validate the effectiveness of IMBMFITFF. First, it is important to investigate the effects of IMBMFITFF in vivo using large animal models. Additionally, combining markers such as STRO-1 and VCAM-1 to examine BMSCs could provide valuable insights. Understanding the molecular mechanisms through which bone marrow significantly enhances the osteogenic activity of the IM is also crucial. Moreover, multicenter studies with larger sample sizes and long-term follow-up periods are needed to validate the clinical applications. Finally, determining the optimal amount of bone marrow fluid required for the most effective IMBMFITFF would be a valuable contribution to the field.

Conclusion

In this paper, we have demonstrated that bone marrow fluid can enhance the osteogenic activity of IMs, leading to SO; the amount of IMSO correlated with the amount of bone marrow fluid. The faster healing of the IMSO-induced TFF than the clinical healing of the tibia indicates that IMBMFITFF can provide additional stability and facilitate a faster and better functional recovery without additional material bone grafts and surgical trauma. These findings suggest that IMBMFITFF can be an effective adjunct for the reconstruction of segmental defects of middle and distal tibia treated using IMT, becoming an alternative to classic TFF.

Abbreviations

IM	Induced membrane
SO	Spontaneous osteogenesis
IMSO	Induced membrane spontaneous osteogenesis
IMT	Induced membrane technique
BMSC	Bone mesenchymal stem cell
DTFS	Distal tibiofibular syndesmosis
PMMA	Polymethylmethacrylate
TFF	Tibiofibular fusion
IMBMFITFF	Induced membrane and bone marrow fluid-induced tibiofibular fusion
BMP-2	Bone morphogenetic protein-2
TGF-β1	Transforming growth factor β1
VEGF	Vascular endothelial growth factor
qRT–PCR	Quantitative real-time polymerase chain reaction

Acknowledgements

The authors would like to express their gratitude to EditSprings (https://www.editsprings.cn) for the expert linguistic services provided, and to F. Shen of Wuxi College for the experimental guidance provided.

Author contributions

QY, S D and FB designed the study. X C, QY performed the experiment. X C, X W, Y W and FB performed clinical applications. XC, and FB prepared the manuscript. QY was responsible for revising the manuscript critically for important intellectual content. All authors read and approved the final manuscript.

Funding

Funding for this project was provided by the top medical expert team of (2021)-the "Taihu Talent Program" in Wuxi (2020) (WXTTP-202010), the "Innovation and Entrepreneurship Program for Excellent Doctorate of Wuxi Ninth People's Hospital (WXNPH-SCYB-202102).

Data availability

The data that support the findings for this study are available to other researchers from the corresponding author upon reasonable request.

Declarations

Ethics approval and consent to participate

This experimental study was reviewed and approved by the Institutional Animal Care and Use Committee of Wuxi Ninth People's Hospital (No.

JY-KT20220132, registration date: October 10, 2022). We have adhered to the ARRIVE guidelines and have included the ARRIVE checklist. Our retrospective clinical study received approval from the Review Board of Wuxi Ninth Peopls's Hospital (No. JY-KT2024067, registration date: March 15, 2024) and was performed in accordance with the ethical standards outlined in the 1964 Declaration of Helsinki and its subsequent amendments. Written informed consent for participation in the study was obtained from each patient.

Consent for publication

Written informed consents of publication of any potentially identifiable images or data included in the study were obtained from the individuals (date: July 2024).

Competing interests

All authors have no conflicts of interest to disclose. All authors have. read and approved the final submitted manuscript.

Author details

[1]Department of Orthopaedics, Wuxi Ninth People's Hospital Affiliated to Soochow University, No. 999 Liangxi Road, Wuxi, Jiangsu 214062, China
[2]Department of Orthopaedics, Wuxi Xinwu District Xinrui Hospital, Wuxi 214060, China

Received: 27 July 2024 / Accepted: 31 October 2024
Published online: 27 February 2025

References

1. Lu Y, Lai CY, Lai PJ, Yu YH. Induced membrane technique for the management of segmental femoral defects: a systematic review and meta-analysis of individual participant data. Orthop Surg. 2023;15(1):28–37. https://doi.org/10.1111/os.13604.
2. Wang J, Yin Q, Gu S, Wu Y, Rui Y. Induced membrane technique in the treatment of infectious bone defect: a clinical analysis. Orthop Traumatol Surg Res. 2019;105(3):535–9. https://doi.org/10.1016/j.otsr.2019.01.007.
3. Masquelet AC. Induced membrane technique: pearls and pitfalls. J Orthop Trauma. 2017;31(Suppl 5):S36–38. https://doi.org/.
4. Zhang L, Lu C, Lv Y, Wang X, Guo S, Zhang H. Three-dimensional printing-assisted Masquelet technique in the treatment of calcaneal defects. Orthop Surg. 2021;13(3):876–83. https://doi.org/10.1111/os.12873.
5. Kanczler JM, Ginty PJ, White L, Clarke NM, Howdle SM, Shakesheff KM, Oreffo RO. The effect of the delivery of vascular endothelial growth factor and bone morphogenic protein-2 to osteoprogenitor cell populations on bone formation. Biomaterials. 2010;31(6):1242–50. https://doi.org/10.1016/j.biomaterials.2009.10.059.
6. Wang K, Gao F, Zhang Y, Dai B, Yan X, He X, Mao D, Rui Y. Comparison of osteogenic activity from different parts of induced membrane in the Masquelet technique. Injury. 2023;54(11):111022. https://doi.org/10.1016/j.injury.2023.111022.
7. Klaue K, Knothe U, Anton C, Pfluger DH, Stoddart M, Masquelet AC, Perren SM. Bone regeneration in long-bone defects: tissue compartmentalisation? In vivo study on bone defects in sheep. Injury. 2009;40(4). https://doi.org/10.1016/j.injury.2009.10.043. S95-102.
8. Gruber HE, Gettys FK, Montijo HE, Starman JS, Bayoumi E, Nelson KJ, Hoelscher GL, Ramp WK, Zinchenko N, Ingram JA, Bosse MJ, Kellam JF. Genome-wide molecular and biologic characterization of biomembrane formation adjacent to a methacrylate spacer in the rat femoral segmental defect model. J Orthop Trauma. 2013;27(5):290–7. https://doi.org/10.1097/BOT.0b013e3182691288.
9. Yin Q, Chen X, Dai B, Liu J, Yang Y, Song S, Ding Y. Varying degrees of spontaneous osteogenesis of Masquelet's induced membrane: experimental and clinical observations. BMC Musculoskelet Disord. 2023;4(1):384. https://doi.org/10.1186/s12891-023-06740-z.
10. Magin MN, Aymar M. Orthotopic tibiofibular fusion: indications–technique–results. Unfallchirurg. 1995;98(7):386–91. German.
11. Piatkowski S, Modrzewski K. Tibio-fibular fusion in the treatment of infected and difficult tibial pseudarthroses. Chir Narzadow Ruchu Ortop Pol. 1974;39(6):741–7. Polish.
12. Lim SK, Ho YC, Ling SK, Yung PS. Functional outcome of fusion versus ligament reconstruction in patients with a syndesmosis injury: a narrative review. Asia Pac J Sports Med Arthrosc Rehabil Technol. 2021;25:53–9. https://doi.org/10.1016/j.asmart.2021.05.002.
13. Cornu O, Manon J, Tribak K, Putineanu D. Traumatic injuries of the distal tibiofibular syndesmosis. Orthop Traumatol Surg Res. 2021;107(1S):102778. https://doi.org/10.1016/j.otsr.2020.102778.
14. Henrich D, Seebach C, Nau C, Basan S, Relja B, Wilhelm K, Schaible A, Frank J, Barker J, Marzi I. Establishment and characterization of the Masquelet induced membrane technique in a rat femur critical-sized defect model. J Tissue Eng Regen Med. 2016;10(10):E382–396. https://doi.org/10.1002/term.1826.
15. Paley D, Maar DC. Ilizarov bone transport treatment for tibial defects. J Orthop Trauma. 2000;14(2):76–85. https://doi.org/10.1097/00005131-200002000-00002.
16. Miska M, Schmidmaier G. Diamond concept for treatment of nonunions and bone defects. Unfallchirurg. 2020;123(9):679–86. https://doi.org/0.1007/s00113-020-00843-1.
17. Khaled A, El-Gebaly O, El-Rosasy M. Masquelet-Ilizarov technique for the management of bone loss post debridement of infected tibial nonunion. Int Orthop. 2022;46(9):1937–44. https://doi.org/10.1007/s00264-022-05494-y.
18. Han W, Shen J, Wu H, Yu S, Fu J, Xie Z. Induced membrane technique: advances in the management of bone defects. Int J Surg. 2017;42:110–6. https://doi.org/10.1016/j.ijsu.2017.04.064.
19. Pélissier P, Lefevre Y, Delmond S, Villars F, Vilamitjana-Amedee J. Influences of induced membranes on heterotopic bone formation within an osteoinductive complex. Experimental study in rabbits. Ann Chir Plast Esthet. 2009;54(1):16–20. https://doi.org/10.1016/j.anplas.2008.07.001. French.
20. Catros S, Zwetyenga N, Bareille R, Brouillaud B, Renard M, Amédée J, Fricain JC. Subcutaneous-induced membranes have no osteoinductive effect on macroporous HA-TCP in vivo. J Orthop Res. 2009;27(2):155–61. https://doi.org/10.1002/jor.20738.
21. Lim ZXH, Rai B, Tan TC, Ramruttun AK, Hui JH, Nurcombe V, Teoh SH, Cool SM. Autologous bone marrow clot as an alternative to autograft for bone defect healing. Bone Joint Res. 2019;8(3):107–17. https://doi.org/10.1302/2046-3758.83.BJR-2018-0096.R1.
22. Salamanna F, Contartese D, Nicoli Aldini N, Barbanti Brodano G, Griffoni C, Gasbarrini A, Fini M. Bone marrow aspirate clot: a technical complication or a smart approach for musculoskeletal tissue regeneration? J Cell Physiol. 2018;233(4):2723–232. https://doi.org/10.1002/jcp.26065.
23. Liu Z, Liu Q, Wang M, Zhou C, Guo H, Liang J, Zhang Y. The early posterior cortex pixel value ratio: a novel reliable indicator for distraction osteogenesis. Front Surg. 2023;10:1280332. https://doi.org/10.3389/fsurg.2023.1280332.
24. Lu Y, Wang J, Yang Y, Yin Q. Bone defects are repaired by enhanced osteogenic activity of the induced membrane: a case report and literature review. BMC Musculoskelet Disord. 2021;22(1):447. https://doi.org/10.1186/s12891-021-04317-2.
25. Tetsworth K, Woloszyk A, Glatt V. 3D printed titanium cages combined with the Masquelet technique for the reconstruction of segmental femoral defects: preliminary clinical results and molecular analysis of the biological activity of human-induced membranes. OTA Int. 2019;2(1):e016. https://doi.org/10.1097/OI9.0000000000000016.
26. Knothe UR, Dolejs S, Matthew Miller R, Knothe Tate ML. Effects of mechanical loading patterns, bone graft, and proximity to periosteum on bone defect healing. J Biomech. 2010;43(14):2728–37. https://doi.org/10.1016/j.jbiomech.2010.06.026.
27. Choi IH, Lee SJ, Moon HJ, Cho TJ, Yoo WJ, Chung CY, Park MS. 4-in-1 osteosynthesis for atrophic-type congenital pseudarthrosis of the tibia. J Pediatr Orthop. 2011;31(6):697–704. https://doi.org/10.1097/BPO.0b013e318221ebce.
28. Masquelet AC, Fitoussi F, Begue T, Muller GP. Reconstruction of the long bones by the induced membrane and spongy autograft. Ann Chir Plast Esthet. 2000;45(3):346–53. French.
29. Yang KY, Lee EH. Isolated congenital pseudoarthrosis of the fibula. J Pediatr Orthop B. 2002;11(4):298–301. https://doi.org/10.1097/00009957-200210000-00006.

30. Gupta G, Ahmad S, Mohd Zahid, Khan AH, Sherwani MK, Khan AQ. Management of traumatic tibial diaphyseal bone defect by induced-membrane technique. Indian J Orthop. 2016;50(3):290–6. https://doi.org/10.4103/0019-5413.181780.